Static analysis of parallel robots with compliant joints for in-hand manipulation

Júlia Borràs and Aaron M. Dollar, *Member, IEEE*

***Abstract*— Many robotic hands use compliant joints because they provide several advantages when interacting with objects in unknown environments, but they also modify the relation between external and internal forces and vary the reachable workspace. This work proposes a detailed study of how compliant joints modify the statics of hands, from the point of view of parallel manipulators. The chosen mathematical framework clarifies the role of joint compliance and its effect on the manipulator performance. This framework is then used in an example application to quantify the reduction/increase of torque exerted by the active joints due to the influence of the passive compliant ones for a three fingered hand.**

I. Introduction

Dexterous in-hand manipulation is an important goal for robotics and prosthetics as it greatly expands the utility of the hand past simple grasping and more effectively utilizes the multiple controllable degrees of freedom present in the majority of hands. In general, within-hand manipulation is typically done with the manipulated object held with the fingertips in a precision grasp [1, 2], affording the fingers doing the manipulation the largest number of degrees of freedom and workspace size while maintaining a stable grasp on the object (Fig. 1).

The general hand/object configuration during these types of precision manipulation tasks is, in effect, similar to common parallel mechanisms, in which the fingers become the "legs" and the object the "platform". This observation affords us the ability to utilize the deep literature on the mechanics of parallel mechanisms to analyze within-hand precision dexterous manipulation, enabling, for instance, the manipulable workspace of a given object/hand to be examined for the purposes of design optimization. Related work examining within-hand manipulation in the context of closed chains mechanisms includes [3-7].

Previous work in kinetostatic analysis of parallel mechanisms, however, has not yet substantially considered joint compliance, which is a major feature in many hands. In particular, underactuated hands [8-11], which are promising for both robotics and prosthetics applications because their design reduces weight, cost, and complexity, simplifies the control, and greatly increases durability, commonly utilize compliant joints to reduce the number of actuators and increase the finger adaptability [12]. Compliant passive joints can perform large deflections, which reduces the contact forces when grasping an object. Specially in unknown environments, flexible passive joints can increase the grasping space and reduce the damage produced for an unexpected collision [13]. In addition, mechanisms built with elastic joints offer several other advantages compared to conventional mechanisms: reduction of wear, clearance and backlash, compactness, no need for lubrication, simplified assembly, reduction of the cost of fabrication, etc.

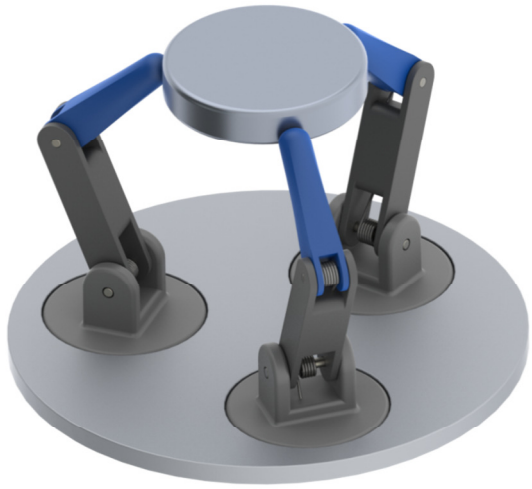

Fig. 1. Three fingers with spring joints manipulating an object can benefit from parallel platforms kinetostatic analysis.

The main objective of the paper is to find a framework to deal with compliant joints to perform a kinetostatic analysis. As far as the authors are aware, there is no detailed study of how the use of compliant joints modifies the relationship between the external forces, the configuration of the system and the torques on the joints for parallel mechanisms. To this end, this work proposes a mathematical framework to deal with fingers with compliant 1-DOF joints when they are manipulating an object. The presented analytical approach is based on parallel robot frameworks [14-16] dealing with compliant joints [17-19]. The developed equations are then applied to an example application in which the reduction or increase of the active joint torques due to the effect of the passive springs are quantified for specific given configurations. While stability analysis and the study of the stiffness matrix are important aspects in the study of compliant parallel manipulators, they are left for future work on the topic.

We begin this paper by discussing how compliance has been treated in the parallel robots literature to date, leading to the presentation of a mathematical framework that clearly defines the role of the passive and the active compliant joints

This work was supported in part by National Science Foundation grant IIS-0952856.

J. Borràs and A. M. Dollar are with the Department of Mechanical Engineering and Materials Science, Yale University, New Haven, CT USA. (e-mail: {julia.borrassol; aaron.dollar}@yale.edu).

(section II). Next, we apply this framework to a 3-URS robot manipulator, a structure equivalent to popular underactuated robotic hands such as the Barrett hand [20, 21] or the JPL hand [21], illustrating how the framework might be used in an example application to analyze the reduction/increase of torque in different configurations due to the action of the springs (section III). Finally, in section IV, we discuss the presented results and directions for future work.

II. Parallel Platforms with Compliant Joints

A. Background and related work

Several models for parallel manipulators with compliant joints have been developed. Many works studying compliant parallel manipulators fall out of the scope of this work because they study the structural rigidity of the mechanism, as any manipulator, even with stiff joints, has a structural compliance that is important for control purposes [22-25]. This is typically done through the study of the stiffness matrix, which can be thought as the Hessian of the potential energy of the system [26].

The static equilibrium equations of the manipulator are usually obtained using the principle of virtual work: *the virtual work done by the applied forces is zero for all the virtual displacements*. It may appear in different equivalent ways [15, 17, 18, 27], because the work done by a constant conservative force ($W = \boldsymbol{F}\,\delta\boldsymbol{x}$) is related to the potential energy through the equation $W = \Delta U$. Then, one can equivalently apply the principle of minimum energy: *a body shall deform or displace to a position that minimizes the total energy*. Even more generally, the same conditions can be obtained using the Lagrangian equations typically used for dynamic models of mechanisms, as done in [18]. Since in the static case the kinetic energy is zero and non-conservative forces are not considered, the Lagrangian equations are equivalent to the minimization of the potential energy.

Usually, the static analysis is part of a general numeric procedure and the provided examples are usually planar manipulators [17, 28-30]. Others study the influence of the external loads on the mechanism configuration [24, 31, 32] but there is still confusion between passive/active compliant joints and the influence of the actuators in the configuration of a compliant mechanism.

B. The joints of a compliant parallel manipulator

Even if all the joints in the fingers of a hand are actuated, once the hand holds an object, close-loop kinematic constraints appear. In the context of parallel manipulators, typically some of the joints are left free to move in order to be able to hold these equations true. These are called passive joints (also called unactuated). A compliant passive joint is also unactuated, but has a spring and thus, it moves in accordance to the applied forces (Fig. 2). Active joints are actuated and thus, they are assumed to be rigid for a given configuration. For compliant active joints we use the definition in [33], that models them as noncompliant actuators connected to a spring, so that they are equivalent to a spring with variable free length. The value of the free length is the commanded value of the actuator. Thus, the torque done by an active joint is modeled as

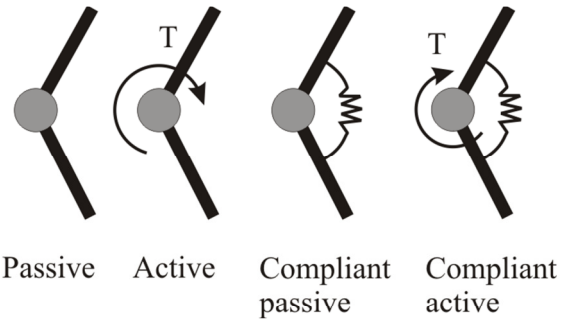

Fig. 2. Passive and active joints with and without compliance. Passive joints are also called unactuated and are free to move. Active joints are controlled by the actuators that exert a torque T. Compliant passive joints exert the torque given by the spring. Compliant active joints exert an actuator torque plus a spring torque.

$$\tau_{\gamma_j} = -k_j(\gamma_j - \psi_j) \tag{1}$$

where γ_j is the angle of the active joint, ψ_j is the commanded value for the actuator in the *j*th active joint and k_j is the stiffness constant of the spring. Note that, (1) can be rewritten into $\tau_{\gamma_j} = -k_j\,\gamma_j + k_j\psi_j$ which is the sum of a torque done by the spring (with 0 length) plus the torque done by the actuator T=$k_j\psi_j$ (Fig. 2).

Using these definitions, a passive joint does not produce force/torque reactions and thus, it does not appear in the static equations. On the contrary, a compliant passive joint exerts force and thus, is typically treated as an active joint [17, 27, 32], without distinguishing between an actuated compliant joint and a passive compliant joint. To the best of the authors' knowledge, this distinction has appeared explicitly in the mathematical formulation only in the Quenouelle and Gosselin works [18, 33].

C. Mathematical formulation

Consider a parallel manipulator with *n* degrees of freedom and *m* joints. The vector of all the joint angles $\boldsymbol{\theta}$ is formed by

$$\boldsymbol{\theta} = (\theta_1, .., \theta_m)^T = (\gamma_1, \dots, \gamma_n, \phi_1, \dots, \phi_c)^T = (\boldsymbol{\Gamma}, \boldsymbol{\phi})^T \tag{2}$$

where the *n* active joints $\boldsymbol{\Gamma} = (\gamma_1, \dots, \gamma_n)$ fully determine the *n* degrees of freedom of the platform. The kinematic constraints are the conditions the joints must hold to maintain the closed kinematic chains, namely

$$\mathrm{K}(\boldsymbol{\Gamma}, \boldsymbol{\phi}) = \mathbf{0}\,, \tag{3}$$

and thus, the *c*= *m*-*n* passive joints can be written in terms of the active as

$$\boldsymbol{\phi} = C(\boldsymbol{\Gamma})\,. \tag{4}$$

For that reason, $\boldsymbol{\phi} = (\phi_1, \dots, \phi_c)$ are also called constrained joints. The relation between the active and passive joints will play an important role in the statics using compliant joints through the matrix $\boldsymbol{G}$ defined as

$$\delta\boldsymbol{\phi} = \boldsymbol{G}\,\delta\boldsymbol{\Gamma}. \tag{5}$$

The position and orientation of the platform are represented by $\boldsymbol{x}$ that can be described with *n* parameters. The forward and inverse kinematic problems consist in obtaining the pose of the platform given the set of

generalized coordinates and vice versa, respectively. This can be done by solving the loop equations:

$$\boldsymbol{x} = L(\boldsymbol{\theta}) = L\big(\boldsymbol{\Gamma},\ C(\boldsymbol{\Gamma})\big). \tag{6}$$

Differentiating the above equation, the Jacobian matrix of a parallel manipulator is obtained, relating the velocity of a point at the platform with the velocities of the active joints,

$$\delta\boldsymbol{\Gamma} = \boldsymbol{J}\,\delta\boldsymbol{x}. \tag{7}$$

For a parallel platform without compliant joints, the principle of virtual work states that the total work done by a wrench applied at the platform must be equal to the total work done by the reaction forces on the active joints, that is

$$\boldsymbol{\tau}_{\boldsymbol{\Gamma}}^{T}\delta\boldsymbol{\Gamma} - \boldsymbol{F}^{T}\delta\boldsymbol{x} = 0, \tag{8}$$

where $\boldsymbol{\tau}_{\boldsymbol{\Gamma}}^{T}$ is the vector of torques exerted by the active joints. The term $\delta\boldsymbol{\Gamma}$ can be substituted using the Jacobian in equation (7) leading to

$$(\boldsymbol{\tau}_{\boldsymbol{\Gamma}}^{T}\boldsymbol{J} - \boldsymbol{F}^{T})\delta\boldsymbol{x} = 0 \Rightarrow\ \boldsymbol{F} = \boldsymbol{J}^{T}\boldsymbol{\tau}_{\boldsymbol{\Gamma}}. \tag{9}$$

Note that this equation expresses the output force on the platform in terms of the actuated joint torques, which means that the platform can resist an external force $-\boldsymbol{F}$. Usually, in the context of parallel robots, the matrix $\boldsymbol{J}^{\mathrm{T}}$ is directly computed using screw theory [16, 34, 35]. Although screw theory may seem an ad hoc methodology, lately there have been several works that show how to use it more systematically [36, 37] .

Consider now the same manipulator with springs in its passive joints. Such passive compliant joints will appear in the static equations because they will exert a force on the platform, and so, they will contribute to the virtual work. Let $\boldsymbol{\tau}_{\boldsymbol{\Gamma}} = \left(\tau_{\gamma_i}\right)^{T}$ be the vector of torques done by the active joints and $\boldsymbol{\tau}_{\boldsymbol{\phi}} = \left(\tau_{\phi_i}\right)^{T}$ the vector of torques done by the passive joints, so that $\boldsymbol{\tau}_{\boldsymbol{\theta}}$ is the vector of all the torques. This means that the term $\boldsymbol{\tau}_{\boldsymbol{\Gamma}}^{T}\delta\boldsymbol{\Gamma}$ in equation (8) is now

$$\boldsymbol{\tau}_{\boldsymbol{\theta}}^{T}\delta\boldsymbol{\theta} = \boldsymbol{\tau}_{\boldsymbol{\Gamma}}^{\mathrm{T}}\delta\boldsymbol{\Gamma} + \boldsymbol{\tau}_{\boldsymbol{\phi}}^{T}\delta\boldsymbol{\phi} = \boldsymbol{\tau}_{\boldsymbol{\Gamma}}^{\mathrm{T}}\delta\boldsymbol{\Gamma} + \boldsymbol{\tau}_{\boldsymbol{\phi}}^{T}\boldsymbol{G}\,\delta\boldsymbol{\Gamma} \tag{10}$$

where $\delta\boldsymbol{\phi}$ has been substituted using equation (5). Then, again using the Jacobian definition in equation (7), the static equilibrium equation in (9) become

$$\big((\boldsymbol{\tau}_{\boldsymbol{\Gamma}}^{\mathrm{T}} + \boldsymbol{\tau}_{\boldsymbol{\phi}}^{T}\boldsymbol{G})\,\boldsymbol{J} - \boldsymbol{F}^{T}\big)\delta\boldsymbol{x} = 0, \tag{11}$$

and thus, the static equations with compliant joints are

$$\boldsymbol{F} = \boldsymbol{J}^{T}\boldsymbol{\tau}_{\boldsymbol{\Gamma}} + \boldsymbol{J}^{T}\boldsymbol{G}^{T}\boldsymbol{\tau}_{\boldsymbol{\phi}}, \tag{12}$$

where for a passive compliant joint i, the magnitude of the torques τ_{ϕ_i} is given by the Hooke's law

$$\tau_{\phi_i} = -k_i(\phi_i - \phi_{i0}) \tag{13}$$

where k_i is the stiffness constant of the spring, ϕ_i is the angle of the passive joint and ϕ_{i0} is the free length of the spring. The active torques $\boldsymbol{\tau}_{\boldsymbol{\Gamma}}$ can be modeled as compliant joints using equation (1). $\boldsymbol{F}$ and $\boldsymbol{\psi} = (\psi_i)^{T}$ for $i = 1, \dots, n$ are called the external parameters and $\boldsymbol{\theta}$ and $\boldsymbol{x}$ the internal parameters of the manipulator.

D. Considerations on compliant versus non-compliant joints

When using compliant active joints, the forward/inverse kinematics must always be solved taking into account the external force applied at the platform. For example, given a desired position $\boldsymbol{x}$, the loop equations in (6) can be solved to find out the corresponding joint angles $\boldsymbol{\theta}$. For any given external force $\boldsymbol{F}$, subtituting the computed values of $\boldsymbol{\theta}$ into equation (12) leads to a linear system for which $\boldsymbol{\tau}_{\Gamma}$ can be computed and finally, the input joint angles $\boldsymbol{\psi} = (\psi_i)^{T}$ that the actuators should command can be obtained through equation (1).

There are two basic static problems, the forward static analysis, which finds the resultant force generated on the platform in a given configuration, and the inverse static analysis, which finds the equilibrium configurations given an external force. For a manipulator with compliant joints, solving the forward static analysis means solving the linear system in (12). For the inverse static problem, given an external force $\boldsymbol{F}$ and the motor inputs $\boldsymbol{\psi}$, the loop equations and the static equations must be solved simultaneously to find the equilibrium configurations $(\boldsymbol{\theta},\ \boldsymbol{x})$.

Observe that the term $\boldsymbol{F} = \boldsymbol{J}^{T}\boldsymbol{\tau}_{\Gamma}$ in equation (12) is the same as the one obtained without compliance in equation (9). Thus, the difference in the static equations when dealing with passive compliant joints is the extra term $\boldsymbol{J}^{T}\boldsymbol{G}^{T}\boldsymbol{\tau}_{\boldsymbol{\phi}}$, let us called it $\boldsymbol{F}^{*}$. $\boldsymbol{F}^{*}$ is a wrench acting on the platform resultant from the torques done by the springs in the passive compliant joints, so, it only depends on the configuration of the manipulator.

If we want to compute the actuation torques the motors have to exert to compensate an external wrench $\boldsymbol{W}$, the output force $\boldsymbol{F}$ in terms of the actuator torques must be $\mathbf{F} = -\mathbf{W}$ and the wrench $\boldsymbol{F}^{*}$ will be subtracted from $\boldsymbol{F}$. That is, for a given configuration, the system in equation (12) is a linear system that can be rewritten as

$$-\boldsymbol{W} - \boldsymbol{F}^{*} = \boldsymbol{J}^{T}\boldsymbol{\tau}_{\boldsymbol{\Gamma}} \tag{14}$$

Using Crammer's rule, the solution of this linear system can be expressed as

$$\tau_{\gamma_j} = \frac{\det\big(\boldsymbol{J}^{j}_{-\boldsymbol{W}-\boldsymbol{F}^{*}}\big)}{\det(\boldsymbol{J})} \tag{15}$$

Where the notation $\boldsymbol{J}_{v}^{j}$ stands for a matrix obtained from $\boldsymbol{J}^{T}$ substituting the jth column by a vector $\boldsymbol{v}$. Using determinant multilinear properties,

$$\tau_{\gamma_j} = \frac{\det\big(\boldsymbol{J}^{j}_{-\boldsymbol{W}}\big)}{\det(\boldsymbol{J})} - \underbrace{\frac{\det\big(\boldsymbol{J}^{j}_{\boldsymbol{F}^{*}}\big)}{\det(\boldsymbol{J})}}_{\tau_j^{*}} \tag{16}$$

where the first term is the torque that would be obtained without passive compliant joints. The above equation means that the torque done by the active joint γ_j, τ_{γ_j}, will be modified by the compliant joints by the extra term τ_j^{*}, that only depends on the configuration of the manipulator and the stiffness constant of the springs. As there is a limit on the torques that the joints can resist, the term τ_j^{*} can change the limits of the reachable workspace.

In conclusion, although both the singularities and the position workspace will remain the same after substituting the joints by spring joints, the reachable workspace will change due to equation (16).

III. CASE STUDY: 3-URS PLATFORM

Consider the manipulator in Fig. 1. It is a 6-DoF manipulator with 3 equal legs with 3 rotational joints each.

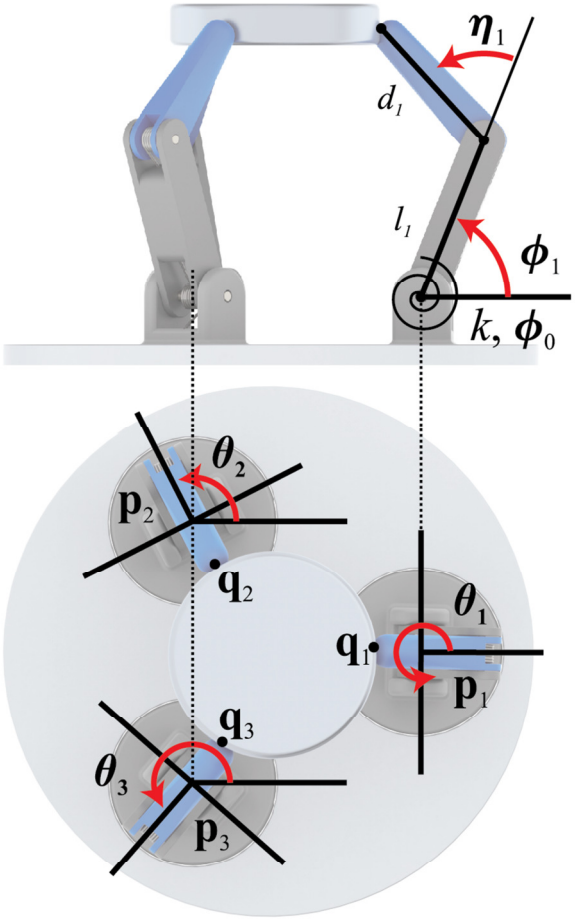

Fig. 3. Description of the joints and the geometry of the manipulator in Fig. 1.

Let $\boldsymbol{z}_{i1} = (0,0,1)^T$ be the axis of rotation of the first joint of leg i, with rotation angle θ_i. The axis of rotation of the second joint is $\boldsymbol{z}_{i2} = (\sin(\theta_i), -\cos(\theta_i), 0)^T$ with a rotation angle ϕ_i. Finally, the third axis is parallel to the previous one, with angle of rotation η_i (see Fig. 3 and 5).

For this example, the angles ϕ_i are left as passive and the active joints are considered without compliance. Then, following equation (2), the active joints are $\boldsymbol{\Gamma} = (\eta_1, \eta_2, \eta_3, \theta_1, \theta_2, \theta_3)^T$ and the passives $\boldsymbol{\phi} = (\phi_1, \phi_2, \phi_3)^T$.

The attachments at the base are named $\boldsymbol{P}_i$ and the corresponding attachment at the platform $\boldsymbol{Q}_i$. Their local coordinates with respect to the center of the base and the center of the platform are

$$\begin{aligned} P_1 &= (a,0,0)^T, \\ P_2 &= \left(-\tfrac{a}{2}, \tfrac{a\sqrt{3}}{2}, 0\right)^T, \\ P_3 &= \left(-\tfrac{a}{2}, -\tfrac{a\sqrt{3}}{2}, 0\right)^T, \\ Q_1 &= (b,0,0)^T, \\ Q_2 &= \left(-\frac{b}{2}, \frac{b\sqrt{3}}{2}, 0\right)^T, \\ Q_3 &= \left(-\tfrac{b}{2}, -\tfrac{b\sqrt{3}}{2}, 0\right)^T. \end{aligned} \tag{17}$$

The parameters a and b define the radius of the base and of the platform.

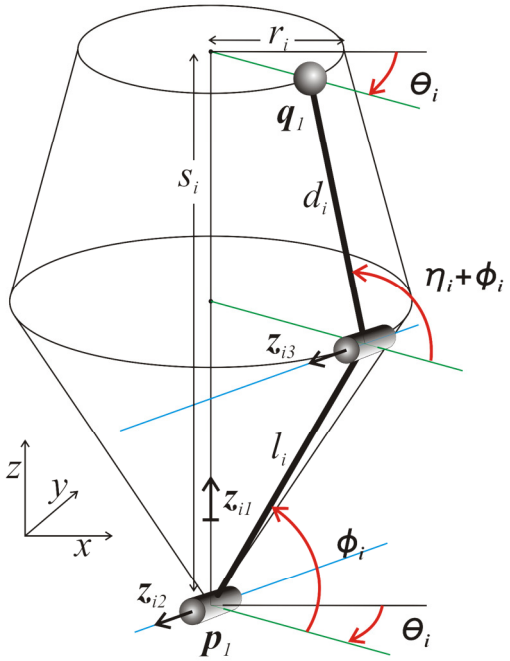

Fig. 4. Points $\boldsymbol{q}_i$ lie always on the circumference at the top of the double cone and thus they can be described as in equation (19).

Let the position and orientation of the platform be given by a position vector $\boldsymbol{p} \in \mathbb{R}^3$ and a rotation matrix $\boldsymbol{R} \in SO(3)$. Then, the coordinates of the attachments with respect to the fixed reference frame located at the center of the base are $\boldsymbol{p}_i = \boldsymbol{P}_i$ and

$$\boldsymbol{q}_i = \boldsymbol{p} + \boldsymbol{R}\,\boldsymbol{Q}_i. \tag{18}$$

On the other hand, the coordinates of the platform attachments can also be parameterized with respect to the angles of rotation of the joint angles following Fig. 4. The point $\boldsymbol{q}_i$ lies always on a circumference at the top of a double cone generated by the revolution of the legs around the axis $\boldsymbol{z}_{i1}$, as shown in Fig. 4. Following this scheme, the coordinates of the platform attachments with respect to the fixed reference frame can be written as

$$\boldsymbol{q}_i = \boldsymbol{p}_i + s_i(0,0,1)^T + r_i(\cos(\theta_i), \sin(\theta_i), 0)^T \tag{19}$$

where

$$\begin{aligned} s_i &= l_i \sin(\phi_i) + d_i \sin(\phi_i + \eta_i), \\ r_i &= l_i \cos(\phi_i) + d_i \cos(\phi_i + \eta_i), \end{aligned} \tag{20}$$

and l_i and d_i are the lengths of the links of the ith leg.

Following the steps in Section II.C, the constraint equations are given by the distance constraints between the platform attachments. Therefore, equation (3) consists of the 3 equations

$$\left(\boldsymbol{q}_i - \boldsymbol{q}_j\right)^2 = 3b^2 \text{ for } i,j = 1,2,3\,, i \neq j. \tag{21}$$

This gives a non-lineal expression of K in (3). As it was not possible to compute the analytical expression of C in equation (4), the matrix $\boldsymbol{G}$ in equation (5) was computed using the chain rule

$$\boldsymbol{G} = \frac{\delta C(\boldsymbol{\Gamma})}{\delta \boldsymbol{\Gamma}} = -\left(\frac{\delta K(\boldsymbol{\theta})}{\delta \boldsymbol{\phi}}\right)^{-1} \frac{\delta K(\boldsymbol{\theta})}{\delta \boldsymbol{\Gamma}}, \tag{22}$$

where equation (4) was used to substitute $\boldsymbol{\phi}$ in (5).

The loop equations in (6) are the 9 equations obtained by equating the platform points computed with respect the

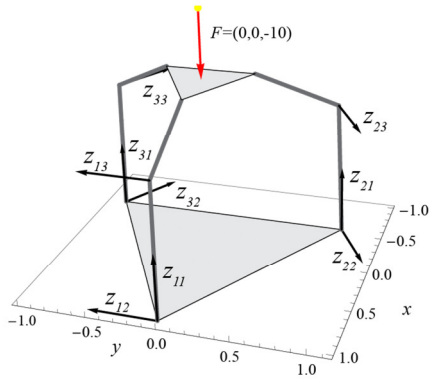

$$\boldsymbol{p} = \begin{pmatrix} 0 \\ 0 \\ 1.3 \end{pmatrix}$$

$$\boldsymbol{R} = \boldsymbol{Id}$$

$$\phi_i = 1.6\ \forall i$$

$$\eta_i = 1.07\ \forall i$$

$$\theta_1 = 0$$

$$\theta_2 = 2.094$$

$$\theta_3 = 4.188$$

Fig. 5. Scheme of the manipulator in a given configuration with a force applied at the center of the platform and the axes of rotation of each leg i andjoint j labeled as $\boldsymbol{z}_{ij}$. On the left side, the position and orientation of the platform are given by the position vector and the rotation matrix, and belowthe corresponding joint angles.

position and orientation of the platform $\boldsymbol{q}_i^x$ (equation (18)) with the same points computed with the angle joints $\boldsymbol{q}_i^a$ (equation (19)). In other words,

$$\boldsymbol{q}_i^x - \boldsymbol{q}_i^a = 0 \text{ for } i = 1,2,3\,. \tag{23}$$

The Jacobian matrix $\boldsymbol{J}^T$can be computed using screw theory following the steps proposed in [15]. Depending on which are the joints chosen as active, different Jacobian matrices are obtained. For this example, the angles ϕ_i are left as passive, thus, the Jacobian matrix is

$$\boldsymbol{J}^T = Diag\left(h_{\eta_1}, h_{\eta_2}, h_{\eta_3}, h_{\theta_1}, h_{\theta_2}, h_{\theta_3}\right)^{-1} \\ (\boldsymbol{\xi}_{\eta_1}, \boldsymbol{\xi}_{\eta_2}, \boldsymbol{\xi}_{\eta_3}, \boldsymbol{\xi}_{\theta_1}, \boldsymbol{\xi}_{\theta_2}, \boldsymbol{\xi}_{\theta_3}). \tag{24}$$

where the screws are defined as

$$\boldsymbol{\xi}_{\theta_i} = (\boldsymbol{z}_{i2}, \boldsymbol{q}_i \times \boldsymbol{z}_{i2})^{\boldsymbol{T}}$$

$$\boldsymbol{\xi}_{\eta_i} = (\boldsymbol{q}_i - \boldsymbol{p}_i, \boldsymbol{q}_i \times (\boldsymbol{q}_i - \boldsymbol{p}_i))^{\boldsymbol{T}},$$

and the elements of the diagonal matrix are

$$h_{\theta i} = -l_i\, cos(\phi_i) - d_i\, cos(\eta_i + \phi_1), \text{ and}$$

$$h_{\eta i} = -l_1 d_i sin(\eta_i).$$

The singularities of the 3-URS manipulator, those positions for which $\det(\boldsymbol{J}) = 0$, are equivalent to the octahedral Stewart-Gough platform and have an easy geometric interpretation (check [38, 39] for more details).

A. *The role of the passive compliant joints*

All the equations have been analytically derived using Wolfram Mathematica 8. For the numerical simulations, we chose dimensions $a = 1, b = 0.375, l_i = 1$ and $d_i = 0.667$, for $i = 1,2,3$. All the lengths are in meters(m) and the angles in radian(rad).

Consider the configuration plotted in Fig. 5. To compute the torques the motors need to exert in each active joint to compensate a given external wrench $\boldsymbol{W}$, we solve the linear system equation (12) with $\boldsymbol{F} = -\boldsymbol{W}$. If the passive joints are not compliant, we solve (9) instead. The stiffness constants for the passive joint springs are set to $k = 2\ \frac{Nm}{rad}$ and the free lengths to $\phi_0 = \pi\ rad$.

For the given configuration, the values of the extra term torques computed using equation (16) are

$$\begin{aligned} \tau_{\eta_1}^* &= -0.712, \\ \tau_{\eta_2}^* &= -0.712, \\ \tau_{\eta_3}^* &= -0.712, \\ \tau_{\theta_1}^* = \tau_{\theta_2}^* &= \tau_{\theta_3}^* = 0, \end{aligned} \tag{25}$$

where the values are all in Nm. That means, for example, that if we put ~1 kg of weight on the platform (an external pure force $\boldsymbol{W} = (0,0,-10\text{N},0,0,0)^{\text{T}}$ is applied), the torques that each actuator has to exert to compensate such force are

Without compliant joints	With compliant joints
$\tau_{\eta_1} = -1.502\ Nm$	$\tau_{\eta_1} = -0.79\ Nm$
$\tau_{\eta_2} = -1.502\ Nm$	$\tau_{\eta_2} = -0.79\ Nm$
$\tau_{\eta_3} = -1.502\ Nm$	$\tau_{\eta_3} = -0.79\ Nm$
$\tau_{\theta_1} = 0\ Nm$	$\tau_{\theta_1} = 0\ Nm$
$\tau_{\theta_2} = 0\ Nm$	$\tau_{\theta_2} = 0\ Nm$
$\tau_{\theta_3} = 0\ Nm$	$\tau_{\theta_3} = 0\ Nm$

So, the overall torque done by the active joints, computed as the sum of the absolute values of each torque, is reduced if the manipulator has passive compliant joints. If we choose a different stiffness constant, k, then the torques for the manipulator using compliant joints are

$$\tau_{\eta_i} = -1.502 + 0.356\, k\ \ Nm$$

and so, we could obtain zero torque on the active joints for a constant of $k = 4.219\,\frac{Nm}{rad}$. Of course, this is only optimum for this configuration and this external force, but optimizing equation (16) over the workspace for a range of forces can help to decide the optimal stiffness constant for the passive joints.

The set of all pure forces of magnitude 10N that can be applied at the center of the platform are plotted in Fig. 6. Each point on the sphere represents the direction of the force, from the point of the sphere to the center of the platform. For each force, if the compliant joints suppose a

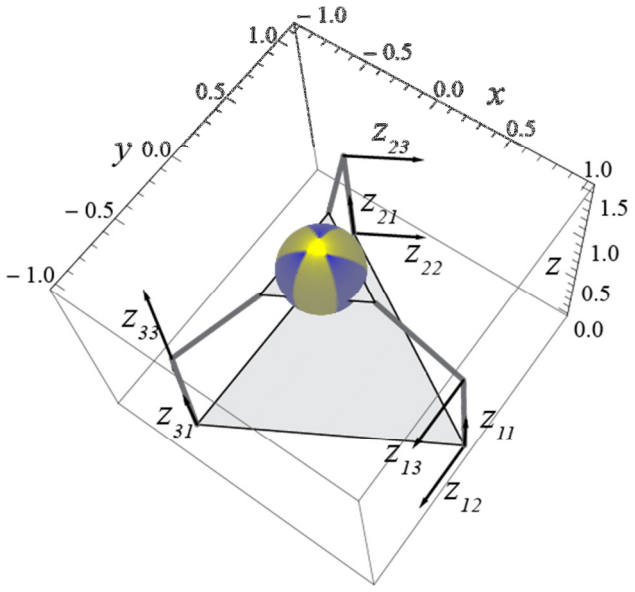

Fig. 6. Each point on the sphere represents a force applied from the point on the sphere to the center of the platform. The range of colors from the lightest (yellow) to the darkest (blue) represent percentages of decrease/increase of the overall torque, from 10% of decrease (lightest/yellow) to 10% of increase (darkest/blue).

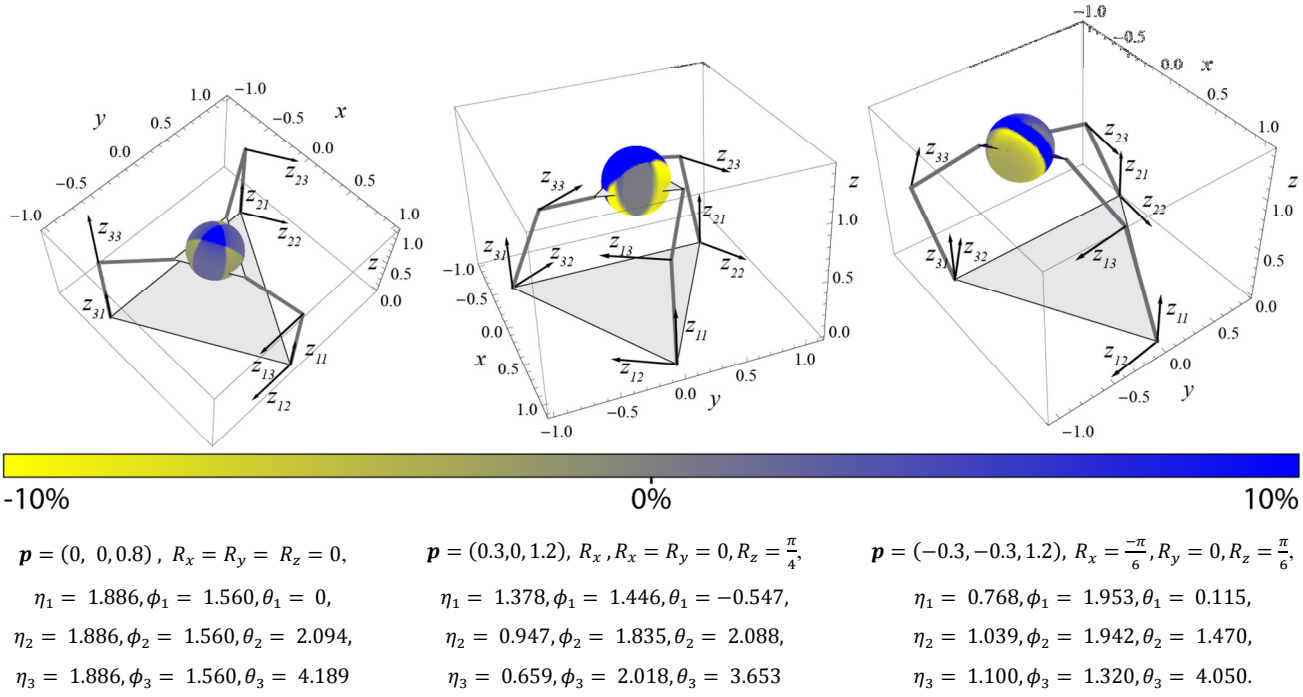

Fig. 7. Representation of all the forces of magnitude 10N applied to the center of the platform for different configurations. The orientation of the platform is given by the rotations around of the *x*, *y* and *z* axis (R_x, R_y, and R_z), and the position vector $\boldsymbol{p}$. Lightest areas (yellow) represent a percentage of decrease of 10% or more of the overall torque, versus darkest areas (blue) that represent an increase of 10% or more.

reduction of the overall torque, the corresponding point is plotted in light color (yellow), on the contrary, in dark color (blue). The colors change from light to dark depending on the percentage of decrease/increase, being the lightest (yellow) if the decrease is equal or bigger than 10%, and the darkest if the increase is 10% or more.

Fig. 7 shows a summary of similar spheres for different configurations of the manipulator. It is shown how the compliant passive joints can help the performance of the manipulator in some directions but not in others. The left figure in Fig. 7 represents the same configuration as in Fig. 6, but with a lower platform height. It shows that, when the angles η_i are bigger than $\pi/2$, the colors are flipped with respect to Fig. 6, but with the same symmetry. Fig 7 central and right show similar computations at different configurations. Away from the center, the symmetry shown before is broken and the ball is split in half light and half dark. This shows that the springs cannot help for all the directions of forces, but the spring parameters can be optimized to help for a specific set of directions.

A more detailed study of the variation of the extra terms τ^* in equation (16) with respect to the location in the workspace is needed to evaluate the impact of using compliant passive joints in the reachable workspace.

IV. Conclusions and Future Work

This work has presented a mathematical framework that clearly distinguishes between active and passive compliant joints. The chosen mathematical formulation shows a promising convenient framework for the future analysis of reachable workspace and manipulability indexes taking into account the presence of active and passive compliant joints.

Using the same framework, the study of underactuation and the stability of the system are future goals that can be addressed through the study of the matrices $\boldsymbol{J}$ and $\boldsymbol{G}$ and through the differentiation of equation (12), respectively.

The quantification of the variation of the torques due to the presence of passive joints has been expressed in an analytical equation that can be used in the future to study the modification of the reachable workspace of the manipulator.

The presented preliminary numerical results show coherent behavior and a promising starting point towards the full comprehension of the role of compliant joints in robotic hands.

References

[1] M. R. Cutkosky, "On grasp choice, grasp models, and the design of hands for manufacturing tasks," *Robotics and Automation, IEEE Transactions on,* vol. 5, pp. 269-279, 1989.

[2] I. M. Bullock and A. M. Dollar, "Classifying human manipulation behavior," in *IEEE International Conference on Rehabilitation Robotics*, 2011, pp. 532-537.

[3] A. Bicchi and D. Prattichizzo, "Manipulability of cooperating robots with unactuated joints and closed-chain mechanisms," *IEEE Transactions on Robotics and Automation,* vol. 16, pp. 336-345, 2000.

[4] C. Rosales, J. M. Porta, R. Suarez, and L. Ros, "Finding all valid hand configurations for a given precision grasp," in *IEEE International Conference on Robotics and Automation*, 2008, pp. 1634-1640.

[5] L. U. Odhner and A. M. Dollar, "Dexterous manipulation with underactuated elastic hands," in *Proceedings of the 2011 IEEE International Conference on Robotics and Automation*, 2011, pp. 5254-5260.

[6] D. Prattichizzo, M. Malvezzi, M. Gabiccini, and A. Bicchi, "On the manipulability ellipsoids of underactuated robotic hands with compliance," *Robotics and Autonomous Systems,* 2011.

[7] J. T. Y. Wen and L. S. Wilfinger, "Kinematic manipulability of general constrained rigid multibody systems," *IEEE Transactions on Robotics and Automation,* vol. 15, pp. 558-567, 1999.

[8] S. Hiroset and Y. Umetani, "The Development of Soft Gripper for the Versatile Robot Hand," *Mechanism and Machine Theory,* vol. 13, pp. 351-359, 1978.

[9] A. Dollar and R. Howe, "The Highly Adaptive SDM Hand: Design and Performance Evaluation," *International Journal of Robotics Research,* vol. 29, pp. 585-597, 2010.

[10] L. Birglen, C. Gosselin, and T. Laliberté, *Underactuated robotic hands* vol. 40: Springer Verlag, 2008.

[11] Y. Kamikawa and T. Maeno, "Underactuated five-finger prosthetic hand inspired by grasping force distribution of humans," in *IEEE/RSJ International Conference on Intelligent Robots and Systems*, 2008, pp. 717-722.

[12] T. Laliberte, L. Birglen, and C. Gosselin, "Underactuation in robotic grasping hands," *Machine Intelligence & Robotic Control,* vol. 4, pp. 1-11, 2002.

[13] A. Dollar and R. Howe, "Towards grasping in unstructured environments: grasper compliance and configuration optimization," *Advanced Robotics,* vol. 19, pp. 523-543, 2005.

[14] J. P. Merlet, *Parallel Robots*, Second Edition. ed.: Springer, 2006.

[15] L. W. Tsai, *Robot analysis: the mechanics of serial and parallel manipulators*: Wiley-Interscience, 1999.

[16] J. K. Davidson, K. H. Hunt, and G. R. Pennock, "Robots and screw theory: applications of kinematics and statics to robotics," *Journal of Mechanical Design,* vol. 126, p. 763, 2004.

[17] H.-J. Su and J. M. McCarthy, "A Polynomial Homotopy Formulation of the Inverse Static Analysis of Planar Compliant Mechanisms," *Journal of Mechanical Design,* vol. 128, p. 776, 2006.

[18] C. Quennouelle and C. Gosselin, "Kinematostatic modeling of compliant parallel mechanisms. Application to a 3-PRRR Mechanism, the Tripteron," *Meccanica,* vol. 46, pp. 155-169, 2011.

[19] C. Quennouelle and C. Gosselin, "A Quasi-Static Model for Planar Compliant Parallel Mechanisms," *Transactions of the ASME Journal of Mechanisms and Robotics,* vol. 1, 2009.

[20] W. Townsend, "The BarrettHand grasper – programmably flexible part handling and assembly," *Industrial Robot: An International Journal,* vol. 27, pp. 181-188, 2000.

[21] J. K. Salisbury and J. J. Craig, "Articulated Hands: Force Control and Kinematic Issues," *The International Journal of Robotics Research,* vol. 1, pp. 4-17, 1982.

[22] M. R. Cutkosky and I. Kao, "Computing and controlling compliance of a robotic hand," *IEEE Transactions on Robotics and Automation,* vol. 5, pp. 151-165, 1989.

[23] N. Simaan and M. Shoham, "Geometric Interpretation of the Derivatives of Parallel Robots' Jacobian Matrix With Application to Stiffness Control," *Journal of Mechanical Design,* vol. 125, pp. 33-42, 2003.

[24] M. Griffis and J. Duffy, "Kinestatic control - a novel theory for simultaneously regulating force and displacement," *Journal of Mechanical Design,* vol. 113, pp. 508-515, 1991.

[25] T. Patterson and H. Lipkin, "Structure of robot compliance," *Journal of Mechanical Design,* vol. 115, pp. 576-576, 1993.

[26] J. Kövecses and J. Angeles, "The stiffness matrix in elastically articulated rigid-body systems," *Multibody System Dynamics,* vol. 18, pp. 169-184, 2007.

[27] J. Duffy, *Statics and kinematics with applications to robotics*: Cambridge Univ Pr, 2007.

[28] C. a. Mattson, L. L. Howell, and S. P. Magleby, "Development of Commercially Viable Compliant Mechanisms Using the Pseudo-Rigid-Body Model: Case Studies of Parallel Mechanisms," *Journal of Intelligent Materials Systems and Structures,* vol. 15, pp. 195-202, 2004.

[29] B. H. Kang, J. T.-y. Wen, N. G. Dagalakis, and J. J. Gorman, "Analysis and Design of Parallel Mechanisms With Flexure Joints," *IEEE Transactions on Robotics,* vol. 21, pp. 1179-1185, 2005.

[30] H. H. Pham and I. m. Chen, "Kinematics , Workspace and Static Analyses of 2-DOF Flexure Parallel Mechanism," in *7th International Conference on Control, Automation, Robotics and Vision.*, 2002, pp. 968-973.

[31] D. Zhang and C. Gosselin, "Kinetostatic modeling of parallel mechanisms with a passive constraining leg and revolute actuators," *Mechanism and Machine Theory,* vol. 37, pp. 599-617, 2002.

[32] A. Pashkevich, A. Klimchik, and D. Chablat, "Enhanced stiffness modeling of manipulators with passive joints," *Mechanism and Machine Theory,* vol. 46, pp. 662-679, 2011.

[33] C. Quennouelle and C. Gosselin, "A Quasi-Static Model for Planar Compliant Parallel Mechanisms," *Journal of Mechanisms and Robotics-Transactions of the Asme,* vol. 1, 2009.

[34] J. P. Merlet, "Singular configurations of parallel manipulators and Grassmann geometry," *The International Journal of Robotics Research,* vol. 8, pp. 45-56, 1989.

[35] D. Kanaan, P. Wenger, S. Caro, and D. Chablat, "Singularity Analysis of Lower Mobility Parallel Manipulators Using Grassmann–Cayley Algebra," *IEEE Transactions on Robotics,* vol. 25, pp. 995-1004, 2009.

[36] J. S. Dai, Z. Huang, and H. Lipkin, "Mobility of overconstrained parallel mechanisms," *Journal of Mechanical Design,* vol. 128, p. 220, 2006.

[37] J. Zhao, B. Li, X. Yang, and H. Yu, "Geometrical method to determine the reciprocal screws and applications to parallel manipulators," *Robotica,* vol. 27, pp. 929-940, 2009.

[38] D. M. Downing, A. E. Samuel, and K. H. Hunt, "Identification of the special configurations of the octahedral manipulator using the pure condition," *The International Journal of Robotics Research,* vol. 21, pp. 147-159, 2002.

[39] J. Angeles, G. Yang, and I. M. Chen, "Singularity analysis of three-legged, six-DOF platform manipulators with URS legs," *IEEE/ASME Transactions on Mechatronics,* vol. 8, pp. 469-475, 2003.